2001; Gan et al., 2004). Although the increased CB in activated microglia of CS−/− mice could compensate for some roles of CS, it may endow them with both phagocytic and neurotoxic capabilities.

In the present study, intrasplenic injection of CFDA and the invasion assay showed that the recruitment and transmigratory abilities of monocytic cells of CS−/− mice were significantly impaired. These results are consistent with the finding that CS degrades major components of the basement membrane of the cerebral vasculature and the leptomeninges including type IV and type V collagens, fibronectin, laminin, vitronectin, and heparan sulfate proteoglycans (Rao et al., 2003). CS has been reported to degrade ECM macromolecules in the brain parenchyma and basement membrane such as proteoglycans, laminin, collagens, elastin, and chondroitin sulfate proteoglycan, even at a neutral pH (Petanceska et al., 1996; Liuzzo et al., 1999). Thus, the impaired migration and recruitment of microglia/monocytic cells are considered mainly responsible for the significant reduction in the mean number of activated microglia accumulated on the axotomized side of the facial motor nuclei of CS−/− mice.

Impairment of Axotomy-Induced Microglial Spreading on Surfaces of Axotomized Facial Motoneurons in CS−/− Mice

There was a marked difference between two groups in the morphology of activated microglia that adhered to injured facial motoneurons. In wild-type mice, activated microglia spread on the surfaces of injured motoneurons. In contrast, CS−/− microglia failed to spread on injured motoneurons and stayed with the relatively large cell bodies. CS deficiency can reasonably be considered responsible for the different morphological changes in activated microglia in CS−/− mice after axotomy because CS can degrade molecules that influence the adhesion properties of microglia.

Perineuronal nets, typically consisting of a chondroitin sulfate proteoglycan complex with hyaluronan and tenascin glycoprotein, are the most conspicuous feature of a specialized neuronal microenvironment. Angelov et al. (1998) reported that TNR in the perineuronal net of motoneurons becomes down-regulated after a peripheral-nerve axotomy. They further showed TNR to be an antiadhesive for microglia. Thus, down-regulation of TNR may make axotomized motoneurons accessible to the stable adhesion of activated microglia, leading to their spreading on the neuronal surface. More recently, a quantitative analysis of vibrissal movement revealed that TNR deficiency promoted functional recovery after a facial nerve axotomy (Guntinas-Lichius et al., 2005). It is likely that down-regulation of TNR and the subsequent adhesion of activated microglia on neuronal surfaces are therefore necessary for the survival and axonal regeneration of axotomized facial motoneurons. In the present study, the amount of TNR in the facial nuclei of CS−/− mice 7 days after axotomy was significantly larger than that in wild-type mice. Axotomy-induced down-regulation of TNR can result from proteolytic degradation by CS secreted from activated microglia. Therefore, insufficient degradation of TNR can reasonably be considered to prevent microglia from spreading on the surfaces of injured motoneurons in CS−/− mice. Additional experiments are needed to further clarify the proteolytic profiles of CS to TNR and other perineuronal nets.

Increase in Axotomy-Induced Motoneuron Death in CS−/− Mice

The rate of neuronal death after a peripheral-nerve axotomy varies significantly between species. In adult rats, the rate of motoneuron death after axotomy is very low, whereas in adult mice, it is relatively high (Ravich et al., 1998; Kiryu-Seo et al., 2005). DBA mice were used in the present study, which showed that a deficiency of CS significantly decreased motoneuron viability in late post-axotomy stages. There are two possible reasons for this decreased neuronal viability in CS−/− mice after axotomy.

One possible explanation is that there is impaired microglial response to axotomy, as CS is known to be exclusively expressed in cells with a monocytic lineage, which include microglia but not neurons. However, there is increasing evidence that microglia do not affect neuronal survival and axonal regeneration. In mouse models deficient in interleukin-6 or macrophage colony-stimulating factor, there was a reduction in the number of microglia during the early response to facial nerve axotomy, but this did not influence the degeneration of facial motoneurons (Galiano et al., 2001; Kalla et al., 2001). To ablate the proliferating microglia, Gowing et al. (2006) recently generated transgenic mice that express a mutant form of herpes simplex virus type 1 thymidine kinase driven by the myeloid-specific CD11b promoter. They showed that specific ablation of proliferating microglia in these transgenic mice could be achieved by the administration of ganciclovir. Using this system, they found that the elimination of proliferating microglia after axotomy did not influence the degeneration of motoneurons after a hypoglossal nerve axotomy.

In contrast, T lymphocytes have been reported to infiltrate into the facial motor nucleus during the early response to a facial nerve axotomy (Galiano et al., 2001; Kalla et al., 2001). Furthermore, the recruited T lymphocytes have been demonstrated to prevent axotomy-induced motoneuron death (Serpe et al., 1999; Byram et al., 2004). Through interactions with T lymphocytes, antigen-presenting cells including microglia are cross-activated. In the present study, we could detect infiltrated CD3-positive T lymphocytes in the facial motor nuclei of wild-type mice but not in those of CS−/− mice following axotomy. CS may also play a role in recruitment of T lymphocytes to the brain parenchyma.

We have previously reported that microglia used CS for the degradation of the invariant chain (Ii) into class II–associated Ii peptide (CLIP; Nishioku et al., 2002; Naka-

nishi, 2003). CS deficiency can reasonably be considered to prevent removal of CLIP from the antigen-binding cleft of MHC II, thus inhibiting antigen presentation to $CD4^+$ T lymphocytes. The expression of MHC II markedly decreased on the axotomized side of the facial motor nuclei of CS−/− mice. Therefore, defective interactions with T lymphocytes may account for the reduced expression of MHC in CS−/− mice after axotomy. However, it was reported that MHC II–positive cells were almost completely limited to perivascular macrophages in a facial axotomy model (Liu et al., 2005). Additional experiments are necessary to elucidate the contribution of defective interaction with T lymphocytes to impaired microglial responses in CS−/− mice after axotomy.

ACKNOWLEDGMENT

We thank Dr. Sandra Ferry (Kyushu University) for providing us with valuable advice in conducting this study.

REFERENCES

Angelov DN, Walther M, Streppel M, Guntinas-Lichius O, Neiss WF, Probstmeier R, Pesheva P. 1998. Tenascin-R is antiadhesive for activated microglia that induce downregulatiuon of the protein after peripheral nerve injury: a new role in neuronal protection. J Neurosci 18:6218–6229.

Bechmann I, Goldmann J, Kovac AD, Kwidzinski E, Simburger E, Naftolin F, Dirnagl U, Nitsch R, Priller J. 2005. Circulating monocytic cells infiltrate layers of anterograde axonal degeneration where they transform into microglia. FASEB J 19:647–649.

Blinzinger K, Kreutzberg GW. 1968. Displacement of synaptic terminals from regenerating motoneurons by microglial cells. Z Zellforsch 85:145–157.

Bromme D, Bonneau PR, Lachance P, Wiederanders B, Krischke H, Peters C, Thomas DY, Storer AC, Vernet T. 1993. Functional expression of human cathepsin S in Saccharomyces cerevisiae. Purification and characterization of the recombinant enzyme. J Biol Chem 268: 4832–4838.

Bromme D, Steinert A, Friebe S, Fittkau S, Wiederanders B, Kirschke H, 1989. The specificity of bovine spleen cathepsin S. Biochem J 264:475–481.

Byram SC, Carson MJ, DeBoy CA, Serpe CJ, Sanders VM, Jones KJ. 2004. CD4-positive T cell-mediated neuroprotection requires dual compartment antigen presentation. J Neurosci 24:4333–4339.

Fujita H, Tanaka J, Toku K, Tateishi N, Suzuki Y, Matsuda S, Sakanaka M, Maeda N. 1996. Effects of GM-CSF and ordinary supplements on the ramification of microglia in culture: a morphological study. Glia 18:269–281.

Galiano M, Liu ZQ, Kalla R, Bohatschek M, Koppius A, Gschwendtner A, Xu S, Werner A, Kloss CUA, Jones LL, Bluethmann H, Raivich G. 2001. Interleukin-6 (IL6) and cellular responses to facial nerve injury: effects on lymphocyte recuitment, early microglial activation and axonal outgrowth in IL6-deficient mice. Eur J Neurosci 14:327–341.

Gan L, Ye S, Chu A, Anton K, Yi S, Vincent VA, von Schack D, Chin D, Murray J, Lohr S, Pattyhy L, Gonzalez-Zulueta M, Nikolich K, Urfer R. 2004. Identification of cathepsin B as a mediator of neuronal death induced by Aβ-activated microglial cells using a functional genomics approach. J Biol Chem 279:205565–205572.

Gowing G, Vallières L, Julien JP. 2006. Mouse model for ablation of proliferating microglia in acute CNS injuries. Glia 53:331–337.

Guntinas-Lichius O, Angelov DN, Morellini F, Lenzen M, Skouras E, Schachner M, Irintchev A. 2005. Opposite impact of tenascin-C and tenascin-R deficiency in mice on the functional outcome of facial nerve repair. Eur J Neurosci 22:2171–2179.

Jinno S, Aika Y, Fukuda T, Kosaka T. 1998. Quantitative analysis of GABAergic neurons in the mouse hippocampus, with optical dissector using confocal laser scanning microscope. Brain Res 814:33–70.

Kalla R, Liu Z, Xu S, Koppius A, Imai Y, Kloss CUA, Kohsaka S, Gschwendtner A, Moller JS, Werner A, Raivich G. 2001. Microglia and early phase of immune surveillance in the axotomized facial motor nucleus: impaired microglial activation and lymphocyte recruitment but no effect on neuronal survival or axonal regeneration in macrophage-colony stimulating factor-deficient mice. J Comp Neurol 436:182–201.

Kingham PJ, Pocock JM. 2001. Microglial secreted cathepsin B induces neuronal apoptosis. J Neurochem 76:1475–1484.

Kiryu-Seo S, Hirayama T, Kato R, Kiyama H. 2005. Noxa is a critical mediator of p53-dependent motor neuron death after nerve injury in adult mouse. J Neurosci 25:1442–1447.

Liu ZQ, Bohatschek M, Pfeffer K, Bluethmann H, Raivich G. 2005. Major histocompatibility complex (MHC2+) perivascular macrophages in the axotomized facial motor nucleus are regulated by receptors for interferon-γ (IFNγ) and tumor necrosis factor (TNF). Neuroscience 131:283–292.

Liuzzo JP, Petanceska S, Moscatelli D, Devi LA. 1999. Inflammatory mediators regulate cathepsin S in macrophages and microglia: a role in attenuating heparan sulfate interactions. Mol Med 5:320–333.

Miyake T, Gahara Y, Nakayama M, Yamada H, Uewabe K, Kitamura T. 1996. Up-regulation of cystatin C by microglia in the rat facial nucleus following axotomy. Mol Brain Res 37:273–282.

Moran LM, Graeber MB. 2004. The facial nerve axotomy model. Brain Res Rev 44:154–178.

Nakanishi H. 2003. Microglial functions and proteases. Mol Neurobiol 27:163–176.

Nakanishi H, Zhang J, Koike M, Nishioku T, Okamoto Y, Kominami E, von Figura K, Peters C, Yamamoto K, Saftig P, Uchiyama Y. 2001. Involvement of nitric oxide released from microglia/macrophages in pathological changes of cathepsin D-deficient mice. J Neurosci 21:7526–7533.

Nakagawa TY, Brissette WH, Lira PD, Griffiths RJ, Petrushova N, Stock J, McNeish JD, Eastmen SE, Howard ED, Clarke SRM, Rosloniec EF, Elliott EA, Rudensky AY. 1999. Impaired invariant chain degradation and antigen presentation and diminished collagen-induced arthritis in cathepsin S null mice. Immunity 19:207–217.

Nishioku T, Hashimoto K, Yamashita K, Liou SY, Kagamiishi Y, Maegawa H, Katsube N, Peters C, von Figura K, Saftig P, Katunuma N, Yamamoto K, Nakanishi H. 2002. Involvement of cathepsin E in exogenous antigen processing in primary cultured murine microglia. J Biol Chem 277:4816–4822.

Petancesk S, Canoll P, Devi LA. 1996. Expression of rat cathepsin S in phagocytic cells. J Biol Chem 271:4403–4409.

Priller J, Flügel A, Wehner T, Boenter M, Hass CA, Prinz M, Fernández-Klett F, Prass K, Bechmann I, de Boer BA, Frotscher M, Kreutzbrg GW, Persons D, Dirnagl U. 2001. Targeting gene-modified hematopoietic cells to the central nervous system: use of green fluorescent protein uncovers microglial engraftment. Nat Med 7:356–1361.

Rao JS. 2003. Molecular mechanisms of glioma invasiveness: the role of proteases. Nat Rev Cancer 3:489–501.

Ravich G, Bohatschek M, Kloss CUA, Werner A, Jones LL, Kreutzberg GW. 1999. Neuroglial activation repertoire in the injured brain: graded response, molecular mechanisms and cues to physiological function. Brain Res Rev 30:77–105.

Raivich G., Gehrmann J, Kreutzberg GW. 1991. Increase of macrophage colony-stimulating factor and granulocyte-macrophage colony-stimulating factor receptors in the regenerating rat facial nucleus. J Neurosci Res 30:682–686.

Ravich G, Jone LL, Kloss CUA, Werner A, Neumann H, Kreutzberg GW. 1998. Immune surveillance in the injured nervous system: T-lymphocytes invade the axotomized mouse facial motor nucleus and aggregate around sites of neuronal degeneration. J Neurosci 18:5804–5816.

Raivich G., Moreno-Flores MT, Moller JC, Kreutzberg GW. 1994. Inhibition of posttraumatic microglial proliferation in a genetic model of macrophage colony-stimulating factor deficiency in the mouse. Eur J Neurosci 6:1615–1618.

Ryan RE, Solane BF, Sameni M, Wood PL. 1995. Microglial cathepsin B: an immunological examination of cellular and secreted species. J Neurochem 65:1035–1045.

Serpe CJ, Kohm AP, Huppenbauer CB, Sanders VM, Jones KJ. 1999. Exacerbation of facial motoneuron loss after facial nerve transction in severe combined immunodeficient (scid) mice. J Neurosci 19:RC7.

Shi GP, Villadangos JA, Dranoff G, Small C, Gu L, Haley KJ, Riese R, Ploegh HL, Chapman HA, 1999. Cathepsin S required for normal MHC class II peptide loading and germinal center development. Immunity 10:197–206.

Shimizu, Hayashi Y, Yamasaki R, Yamada J, Zhang J, Ukai K, Koike M, Mine K, von Figura K, Peters C, Saftig P, Fukuda T, Uchiyama Y, Nakanishi H. 2005. Proteolytic degradation of glutamate decarboxylase mediates disinhibition of hippocampal CA3 pyramidal cells in cathepsin D-deficient mice. J Neurochem 94:680–690.

Streit WJ, Graeber MB, Kreutzberg GW. 1989. Peripheral nerve lesion produces increased levels of major histocompatibility complex antigens in the central nervous system. J Neuroimmunol 21:117–123.

Sukhova GK, Zhang Y, Pan JH, Wada Y, Yamamoto T, Naito M, Kodama T, Tsimikas S, Witztum JL, Lu ML, Sakara Y, Chin MT, Libby P, Shi GP. 2003. Deficiency of cathepsin S reduces atherosclerosis in LDL receptor-deficient mice. J Clin Invest 111:897–906.

Uwabe K, Gahara Y, Yamada H, Miyake T, Kitamura T. 1997. Identification and characterization of a novel gene (neurorep 1) expressed in nerve cells and up-regulated after axotomy. Neuroscience 80:501–509.

ANTIMICROBIAL AGENTS AND CHEMOTHERAPY, June 2007, p. 2274–2277 Vol. 51, No. 6
0066-4804/07/$08.00+0 doi:10.1128/AAC.00917-06

Prophylactic Effect of Dietary Seaweed Fucoidan against Enteral Prion Infection[▽]

Katsumi Doh-ura,[1]* Tomoko Kuge,[2] Miyuki Uomoto,[1] Keiko Nishizawa,[1] Yuri Kawasaki,[1] and Masahiko Iha[3]

Department of Prion Research, Tohoku University Graduate School of Medicine, Sendai, Japan[1]; Department of Neuropathology, Graduate School of Medical Sciences, Kyushu University, Fukuoka, Japan[2]; and South Product Ltd., Okinawa, Japan[3]

Received 25 July 2006/Returned for modification 25 August 2006/Accepted 28 March 2007

Dietary seaweed fucoidan delays the onset of disease of enterally infected mice with scrapie when given orally for 6 days after infection, but not when given before the infection. This effect was not modified at a tested fucoidan dose range and appeared to reach the maximum level at a concentration of 2.5% or less in feed. Daily uptake of fucoidan might be prophylactic against prion diseases caused by ingestion of prion-contaminated materials, although further evaluation of its pharmacology remains to be done.

Transmissible spongiform encephalopathies, or prion diseases, are fatal neurodegenerative disorders that include Creutzfeldt-Jakob disease (CJD) and Gerstmann-Sträussler-Scheinker syndrome in humans and scrapie, bovine spongiform encephalopathy (BSE), and chronic wasting disease in animals. Recent outbreaks of BSE and variant CJD (vCJD), both of which are considered to occur through ingestion of BSE-contaminated materials (reviewed in reference 21), have necessitated the development of preventive measures against these diseases.

Sulfated polysaccharides, such as heparin, dextran sulfate, and pentosan polysulfate (PPS), are known either to prolong incubation periods in animals with prion diseases or to inhibit formation of pathogen-related abnormal prion protein (PrP) in prion-infected cells (reviewed in reference 3). Their therapeutic effects are attributed to inhibition of the conversion of normal PrP to abnormal PrP by either competitively binding to the normal PrP (4) or reducing normal PrP on the cell surface through stimulation of endocytosis (20). These large-molecule compounds are not taken up well from the gut to blood or from blood to the brain (a target organ of prion diseases). Therefore, these compounds are effective in cases of peripheral infection when given intraperitoneally, intravenously, or subcutaneously (8) and even in cases of intracranial infection when given intracerebroventricularly (5). Recently, PPS intracerebroventricular injection has been utilized for clinical trials of patients; the clinical outcome remains to be determined (17).

Fucoidans, complex sulfated fucosylated polysaccharides, are known to have various biological activities: anticoagulant, antiviral, antiparasital, anti-inflammatory, contraceptive, and so on, because of their ability to imitate patterns of sulfate substitution on glycosaminoglycans and other sulfated glycans (2). Some fucoidans are present in large quantities in dietary brown seaweed food products, which are eaten frequently in Asian countries (9). Here, we report that fucoidan from popularly eaten brown algae has antiprion activity and delays disease onset when it is ingested after the enteral prion infection.

Fucoidan was prepared from the brown seaweed *Cladosiphon okamuranus* Tokida (Fig. 1A) and subsequently tested as described previously (15). Briefly, the brown seaweed was suspended in distilled water adjusted to pH 3.0 with 30% HCl and heated at 100°C for 30 or 60 min. The suspension was centrifuged (10,000 × *g*) at room temperature, and the supernatant was filtered using Microza UF membrane (Asahi Kasei Chemicals, Japan). Then the retentate was washed with distilled water and lyophilized. The levels of fucose, uronic acid, and sulfate in the lyophilized preparation were determined by examining the results of the phenol-H_2SO_4 reaction and carbazole reaction and by ion chromatography, respectively. The purity and molecular mass of the lyophilized preparation were determined by gel filtration high-performance liquid chromatography. Two fucoidan preparations were used in the experiment: sample 1, with an average mass of 42.6 kDa and 87.8% fucoidan content; and sample 2, with an average mass of 140.4 kDa and 87.1% fucoidan content.

Inhibition of abnormal PrP synthesis in vitro was investigated as described previously (7, 12) in three different prion-infected neuroblastoma (NB) cells, each of which was persistently infected with a distinct prion strain from scrapie (RML or 22L) or human prion disease (Fukuoka-1). The cells were cultured for 3 days in the presence of fucoidan, and proteinase K-resistant abnormal PrP in the cell lysate was recovered by ultracentrifugation and analyzed by immunoblotting with three different anti-PrP antibodies, SAF83 against human PrP142-160 (SPI-BIO, France), PrP-2B against mouse/hamster PrP89-103 (5), and PrP-3B against mouse/hamster PrP218-232 (not published). The three antibodies produced the same immunoblot data in the following studies. Therefore, all immunoblot figures presented are of SAF83. The results from prion-infected NB cells showed that sample 2 of the higher-molecular-mass fucoidan more strongly inhibited abnormal PrP formation at half-maximum effective dosages ranging from 2.5 μg/ml to 5.0 μg/ml in all cells (Fig. 1B), suggesting that fucoidan exerts its antiprion activity in a prion strain-independent manner. The inhibition was irreversible, and even the most effective

* Corresponding author. Mailing address: Department of Prion Research, Tohoku University Graduate School of Medicine, 2-1 Seiryo-cho, Aoba-ku, Sendai, Miyagi 980-8575, Japan. Phone: 81-22-717-8232. Fax: 81-22-717-7656. E-mail: doh-ura@mail.tains.tohoku.ac.jp.

▽ Published ahead of print on 16 April 2007.

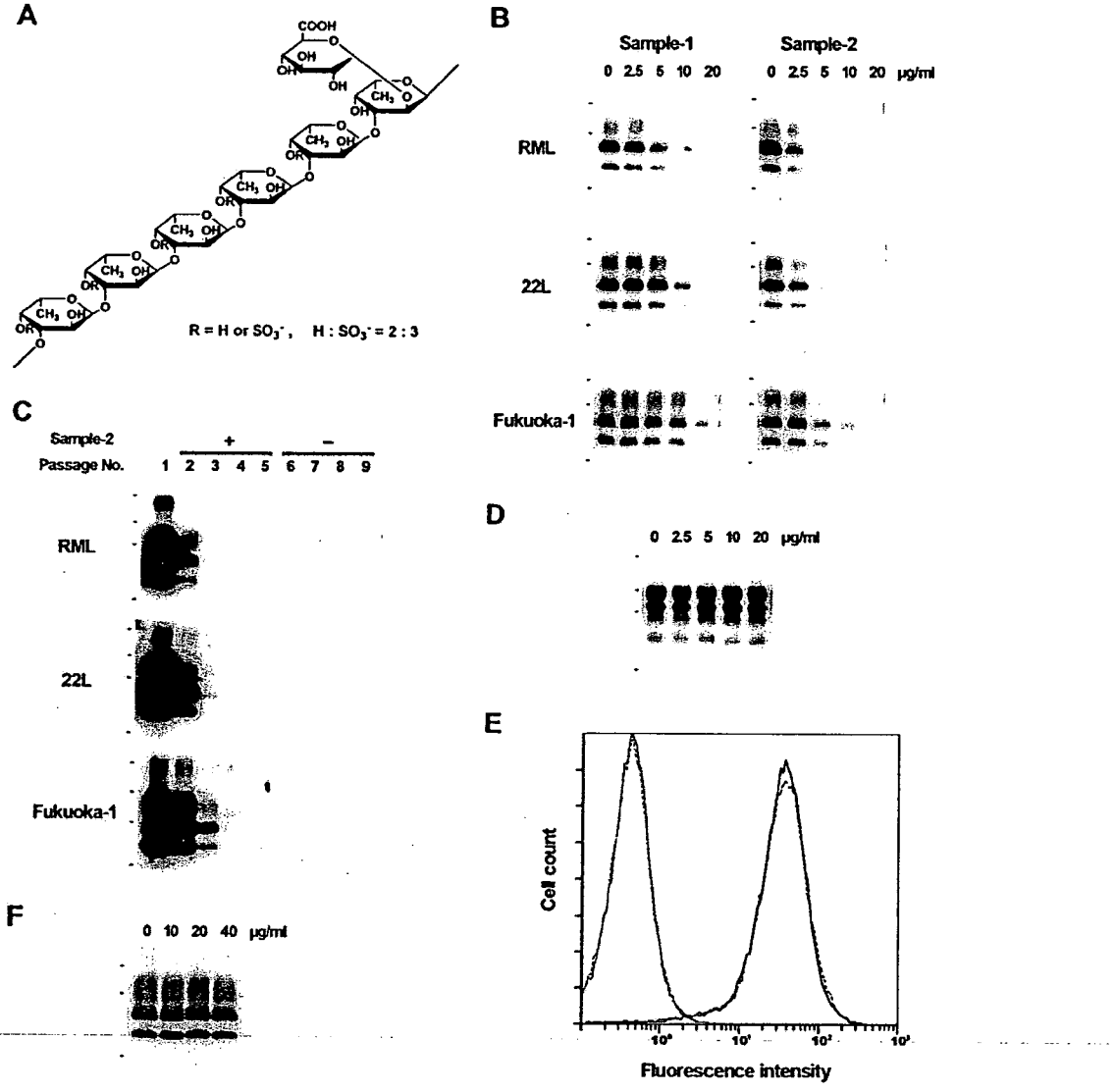

FIG. 1. Fucoidan and its effects on prion-infected or noninfected cells. (A) Chemical structure of fucoidan from *Cladosiphon okamuranus* Tokida. (B) Immunoblot analyses of abnormal PrP in the prion-infected NB cells treated with fucoidan. The small black bars to the left of the blots indicate the positions of molecular size markers at 42, 32, and 17 kDa. (C) Immunoblot analyses of abnormal PrP in the prion-infected NB cells serially passaged in the presence (+) and subsequently in the absence (−) of fucoidan. Overexposed images are shown. The small black bars to the left of the blots indicate the positions of molecular size markers at 81, 42, 32, and 17 kDa. (D) Immunoblot analysis of total normal PrP in noninfected NB cells treated with fucoidan. The molecular size markers to the left of the blot are the same as in panel C. (E) Flow cytometric analysis of normal PrP on the cell surface in noninfected NB cells treated with fucoidan. The solid line and broken line indicate fucoidan-treated cells and nontreated cells, respectively. Gray line peaks on the left show their respective isotype controls. (F) Immunoblot analysis of abnormal PrP from RML-infected cell lysate incubated with fucoidan prior to protease digestion. The molecular size markers to the left of the blot are the same as in panel B. All immunoblot data shown here are of SAF83.

abnormal PrP preparation technique, sodium phosphotungstic acid precipitation (18), never demonstrated that abnormal PrP signals that had once disappeared after treatment with 10 μg/ml of sample 2 fucoidan could reappear after serial passages in the absence of fucoidan (Fig. 1C). The inhibition mechanism included no alteration of either the total or cell surface level of normal PrP. That fact was demonstrated in noninfected NB cells treated with 20 μg/ml sample 2 fucoidan by either immunoblot analysis of the cell lysate without protease digestion or flow cytometric analysis performed as described previously (6) (Fig. 1D and E). In addition, apparent modification of the abnormal PrP with fucoidan was not observed in the immunoblot data when the RML-infected cell lysate was incubated with 20 μg/ml sample 2 fucoidan at 37°C for 1 h and processed to obtain the abnormal PrP as described (Fig. 1F). The findings are consistent with those of heparan sulfate mimetics (1, 19), but not those of PPS and dextran sulfate, which stimulate endocytosis of normal PrP on the cell surface and engender reduction of the total and cell surface normal PrP (20). Thus, reduction of normal PrP is not neces-

TABLE 1. Antiprion effects of fucoidan mixed with infectious inoculum

Expt no.	Fucoidan concn in inoculum (μg/ml)	Incubation period (days) (mean ± SD) (n^c)	Statistical significance
Expt 1[a]	200	57.9 ± 2.5 (8)	$P < 0.05^d$
	20	55.0 ± 2.5 (6)	
	2	54.2 ± 2.7 (5)	
	0.2	54.2 ± 3.9 (6)	
	0.02	53.7 ± 2.6 (6)	
	0 (control)	53.0 ± 2.7 (6)	
Expt 2[b]	200	73.3 ± 3.7 (7)	$P < 0.01^e$
	20	67.4 ± 7.2 (5)	
	2	69.0 ± 2.1 (5)	
	0.2	66.8 ± 4.6 (6)	
	0.02	64.4 ± 4.5 (7)	
	0 (control)	62.2 ± 2.2 (6)	

[a] Twenty microliters of 1% 263K prion homogenate mixed with the designated dose of sample 2 fucoidan was inoculated intracerebrally into each Tg7 mouse immediately after the mixture was made.
[b] Twenty microliters of 0.1% 263K prion homogenate with the designated dose of sample 2 fucoidan was inoculated intracerebrally into each Tg7 mouse after the mixture was incubated for 14 h at room temperature.
[c] Number of mice tested in each group.
[d] Statistical significance against the value for the control, analyzed using one-way analysis of variance followed by the Tukey-Kramer method for multiple comparisons.
[e] Statistical significance against the value for either the 0.02 μg/ml group or the control, analyzed as described in footnote *d*.

TABLE 2. Prophylactic effects of fucoidan feeding preinfection or postinfection

Time of feeding	Fucoidan concn in feed (%)	Incubation period (days) (mean ± SD) (n^c)	Statistical significance
Preinfection[a]	2.5	215.4 ± 40.5 (5)	
	5	243.4 ± 31.8 (5)	
	10	212.2 ± 37.7 (5)	
Postinfection[b]	2.5	346.8 ± 28.0 (5)	$P < 0.01^d$
	5	368.1 ± 73.9 (7)	$P < 0.01^d$
	10	367.4 ± 44.9 (5)	$P < 0.01^d$
Control		231.1 ± 28.3 (6)	

[a] Fucoidan feeding started 7 days prior to enteral inoculation by gavage feeding with 200 μl of 10% 263K prion homogenate and ended the day before inoculation.
[b] Fucoidan feeding started the day after enteral inoculation and continued for 6 days.
[c] Number of mice tested in each group.
[d] Statistical significance against either the value for the preinfection group or the control, analyzed as described in Table 1, footnote *d*.

sarily responsible for the antiprion action of sulfated polysaccharides.

In one antiprion in vivo test, prion homogenate was mixed with a test compound prior to intracerebral inoculation and injected into the animal brain to elucidate increased incubation times attributable either to inactivation of the inoculum or its presence in the brain at the time of infection. Sample 2 was more effective in vitro. Therefore, it was tested in this manner using an animal model comprising hamster scrapie prion strain 263K and Tg7 mice expressing hamster PrP (16). That model was chosen because it gives the shortest incubation times of all experimental animal models available and because antiprion activity of fucoidan was observed, irrespective of prion strains. In an initial experiment, immediately after 20 μl of 1% 263K prion homogenate equivalent to an infectivity titer of about 10^8 50% lethal dose (LD_{50})/g of tissue (5) was mixed with sample 2 fucoidan at its final concentration of 0 to 200 μg/ml, five to eight-week-old Tg7 mice per group were inoculated intracerebrally with the mixture. Only the mixture containing the largest amount of sample 2 significantly increased the incubation period ($P < 0.05$) compared to that of the control (experiment 1 in Table 1).

Next, to determine whether preincubation of the mixture enhances inactivation of the infectious inoculum, the prion homogenate-fucoidan mixtures, similarly prepared but containing 10 times more diluted homogenate, were incubated for 14 h at room temperature and then injected similarly into five to seven mice per group. Experiment 2 in Table 1 shows that only the mixture containing the largest amount of sample 2 significantly increased the incubation period ($P < 0.01$), as demonstrated similarly in experiment 1. The findings suggest that fucoidan itself does not modify infectivity of the inoculum, but its presence in the brain might inhibit prion replication or PrP conversion, probably in a manner similar to that observed in vitro. This inference is supported by results described in previous reports that PPS is effective in delaying the onset of disease of prion-infected animals when administered continuously into the brain (5) or even by bolus shots (13). However, there remains another possibility, the possibility that fucoidan can modify the infectivity in the inoculum very rapidly without a 14-h incubation.

Finally, the potential practical utility of fucoidan was investigated, especially its prophylactic effects against peroral and enteral prion infections such as those that occur in BSE and vCJD. Two different timings of fucoidan feeding, where fucoidan powder was given in a mixture with feed powder at three different levels (2.5, 5, or 10%) were designed to reveal its distinct effects in mice. In one, fucoidan feeding started 7 days prior to enteral inoculation into five to seven Tg7 mice per group by gavage feeding over a few hours with a total of 200 μl of 10% 263K prion homogenate (about 10^9 LD_{50}/g infectivity titer) and ended the day preceding inoculation to elucidate its preinfection prophylactic effects. In the other, fucoidan feeding started the day after the inoculation and continued for 6 days to elucidate its postinfection prophylactic effects. The results demonstrated that fucoidan feeding that commenced after the enteral inoculation delayed the disease onset for about half the time of the control incubation (Table 2). However, fucoidan feeding before the enteral inoculation did not affect the incubation time.

Low proportions of fucoidan are absorbed from the gut into blood (11) and excreted in urine (10), although little more is known of the detailed pharmacology of ingested fucoidan. Sulfated polysaccharides injected intraperitoneally or intravenously inhibit prion replication in the lymphoreticular system, which is involved in the delivery of prion from the gut to the brain (8, 14). Therefore, it can be speculated that fucoidan absorbed into blood exerts its effects by inhibiting prion replication in the lymphoreticular system. A gap of fucoidan effects between the preinfection and postinfection fucoidan feeding might be attributable to the rapid clearance of blood fucoidan

into urine when this is the case. Another possible mechanism of the postinfectious fucoidan effects might be that it facilitates the excretion of infectious materials from the gut. This inference is supported by the fact that seaweed polysaccharides and other natural polysaccharides alter the bacterial spectrum of the gut and assist detoxification (9). In contrast, fucoidan does not seem to act via a certain factor induced in the host because fucoidan administered until the day before inoculation was never effective.

There was no difference in prolonged incubation times among the three different fucoidan concentrations, although the feed consumption per mouse was not statistically different in each experimental group irrespective of the fucoidan level. This might occur because even the lowest concentration of fucoidan in feed surpasses its absorption threshold from the gut or because blood fucoidan concentrations are not parallel to ingested fucoidan doses. The latter was previously reported in humans, where only a threefold difference in blood plasma fucoidan concentrations was detected despite a 7.5-fold difference in ingested fucoidan doses (11). In addition, the stoichiometric relationship between blood fucoidan concentration and inhibitory activity against prion replication in vivo might also be attributable to the results observed here. However, these inferences remain to be elucidated.

The inoculum used in the study of enteral infection contained an extremely high titer of about 10^9 LD_{50}/g, although most of the inoculum might be excreted in feces, and presumably, a much lower titer may cause the infection. More satisfactory prophylactic effects by orally ingested fucoidan might be expected when prion infection in BSE or vCJD is presumed to occur through a lower level of infectivity than that used in this study. On the other hand, the data presented cannot exclude the possibility that the in vivo effects of fucoidan on the 263K prion strain are different from those on other strains. However, this did not occur during our previous experiments with a sulfated polysaccharide (5).

Finally, all fucoidan samples used here contained fucoidan at less than 90% of total weight. Therefore, it is possible that ingredients other than fucoidan exert the antiprion activity observed in this study. However, gel-filtrated samples, which contained 99.9% fucoidan with a mass of 100 to 190 kDa produced the same in vitro results (data not shown). Therefore, fucoidan itself of the dietary brown seaweed imparts the antiprion activity. Its daily ingestion has the potential to provide some prophylactic benefit against such oral or enteral prion infections as occurred in BSE and vCJD, but further studies must be done to elucidate the pharmacology of ingested fucoidan.

This work was supported by the Ministry of Health, Labor and Welfare (H16-kokoro-024) and the BSE Control Project of the Ministry of Agriculture, Forestry and Fisheries of Japan.

We thank Satoshi Kawatake for valuable suggestions and Kyomi Sasaki for manuscript preparation.

REFERENCES

1. **Adjou, K. T., S. Simoneau, N. Salès, F. Lamoury, D. Dormont, D. Papy-Garcia, D. Barritault, J. P. Deslys, and C. I. Lasmézas.** 2003. A novel generation of heparan sulfate mimetics for the treatment of prion diseases. J. Gen. Virol. 84:2595–2603.
2. **Berteau, O., and B. Mulloy.** 2003. Sulfated fucans, fresh perspectives: structures, functions, and biological properties of sulfated fucans and an overview of enzymes active toward this class of polysaccharide. Glycobiology 13:29R–40R.
3. **Cashman, N. R., and B. Caughey.** 2004. Prion diseases–close to effective therapy? Nat. Rev. Drug Discov. 3:874–884.
4. **Caughey, B., K. Brown, G. J. Raymond, G. E. Katzenstein, and W. Thresher.** 1994. Binding of the protease-sensitive form of PrP (prion protein) to sulfated glycosaminoglycan and Congo red. J. Virol. 22:163–167.
5. **Doh-ura, K., K. Ishikawa, I. Murakami-Kubo, K. Sasaki, S. Mohri, R. Race, and T. Iwaki.** 2004. Treatment of transmissible spongiform encephalopathy by intraventricular drug infusion in animal models. J. Virol. 78:4999–5006.
6. **Doh-ura, K., K. Tamura, Y. Karube, M. Naito, T. Tsuruo, and Y. Kataoka.** 19 January 2007. Chelating compound, chrysoidine, is more effective in both antiprion activity and brain endothelial permeability than quinacrine. Cell. Mol. Neurobiol. doi:10.1007/s10571-006-9122-0.
7. **Doh-Ura, K., T. Iwaki, and B. Caughey.** 2000. Lysosomotropic agents and cysteine protease inhibitors inhibit scrapie-associated prion protein accumulation. J. Virol. 74:4894–4897.
8. **Farquhar, C., A. Dickinson, and M. Bruce.** 1999. Prophylactic potential of pentosan polysulphate in transmissible spongiform encephalopathies. Lancet 353:117.
9. **Fitton, J. H.** 2003. Brown marine algae: a survey of therapeutic potentials. Altern. Complem. Ther. 9:29–33.
10. **Guimarães, M. A. M., and P. A. S. Mourão.** 1997. Urinary excretion of sulfated polysaccharides administered to Wistar rats suggests a renal permselectivity to these polymers based on molecular size. Biochim. Biophys. Acta 1335:161–172.
11. **Irhimeh, M. R., J. H. Fitton, R. M. Lowenthal, and P. Kongtawelert.** 2005. A quantitative method to detect fucoidan in human plasma using a novel antibody. Methods Find. Exp. Clin. Pharmacol. 27:705–710.
12. **Ishikawa, K., Y. Kudo, N. Nishida, T. Suemoto, T. Sawada, T. Iwaki, and K. Doh-ura.** 2006. Styrylbenzoazole derivatives for imaging of prion plaques and treatment of transmissible spongiform encephalopathies. J. Neurochem. 99:198–205.
13. **Kocisko, D. A., W. S. Caughey, R. E. Race, G. Roper, B. Caughey, and J. D. Morrey.** 2006. A porphyrin increases survival time of mice after intracerebral prion infection. Antimicrob. Agents Chemother. 50:759–761.
14. **Mabbott, N. A., and G. G. MacPherson.** 2006. Prions and their lethal journey to the brain. Nat. Rev. Microbiol. 4:201–211.
15. **Nagaoka, M., H. Shibata, I. Kimura-Takagi, S. Hashimoto, K. Kimura, T. Makino, R. Aiyama, S. Ueyama, and T. Yokokura.** 1999. Structural study of fucoidan from *Cladosiphon okamuranus Tokida*. Glycoconjugate J. 16:19–26.
16. **Race, R. E., S. A. Priola, R. A. Bessen, D. Ernst, J. Dockter, G. F. Rall, L. Mucke, B. Chesebro, and M. B. Oldstone.** 1995. Neuron-specific expression of a hamster prion protein minigene in transgenic mice induces susceptibility to hamster scrapie agent. Neuron 15:1183–1191.
17. **Rainov, N. G., I. R. Whittle, and K. Doh-ura.** 2005. Treatment options in patients with prion disease—the role of long term cerebroventricular infusion of pentosan polysulphate, p. 41–66. *In* T. Kitamoto (ed.), Prions—food and drug safety. Springer-Verlag, Tokyo, Japan.
18. **Safar, J., H. Wille, V. Itri, D. Groth, H. Serban, M. Torchia, F. E. Cohen, and S. B. Prusiner.** 1998. Eight prion strains have PrP^{Sc} molecules with different conformations. Nat. Med. 4:1157–1165.
19. **Schonberger, O., L. Horonchik, R. Gabizon, D. Papy-Garcia, D. Barritault, and A. Taraboulos.** 2003. Novel heparan mimetics potently inhibit the scrapie prion protein and its endocytosis. Biochem. Biophys. Res. Commun. 312:473–479.
20. **Shyng, S. L., S. Lehmann, K.L. Moulder, and D. A. Harris.** 1995. Sulfated glycans stimulate endocytosis of the cellular isoform of the prion protein, PrP^{C}, in cultured cells. J. Biol. Chem. 270:30221–30229.
21. **Taylor, D. M.** 2002. Current perspectives on bovine spongiform encephalopathy and variant Creutzfeldt-Jakob disease. Clin. Microbiol. Infect. 8:332–339.

Cellular and Molecular Neurobiology, Vol. 27, No. 3, May 2007 (© 2007)
DOI: 10.1007/s10571-006-9122-0

Chelating Compound, Chrysoidine, Is More Effective in Both Antiprion Activity and Brain Endothelial Permeability Than Quinacrine

Katsumi Doh-ura,[1,5] Kazuhiko Tamura,[2] Yoshiharu Karube,[3] Mikihiko Naito,[4] Takashi Tsuruo,[4] and Yasufumi Kataoka[2]

Received July 26, 2006; accepted September 27, 2006; Published online: January 19, 2007

SUMMARY

1. As an extension of our previous study of quinacrine and its derivatives, chelating chemicals were screened to obtain more effective, better brain-permeable antiprion compounds using either prion-infected neuroblastoma cells or brain capillary endothelial cells.

2. Eleven chemicals were found to have antiprion activity. Most of them shared a common structure consisting of benzene or naphthalene at either end of an azo bond. Structure–activity data suggest that chelating activity is not necessary but might contribute to the antiprion action.

3. Chrysoidine, a representative compound found here, was about 27 times more effective in the antiprion activity and five times more efficiently permeable through the brain capillary endothelial cells than quinacrine was.

4. These chemicals might be useful as compounds for development of therapeutics for prion diseases.

KEY WORDS: prion; chrysoidine; blood–brain barrier; aromatic azo compounds; therapy; chelating agents; brain endothelial cells; prion-infected neuroblastoma cells.

INTRODUCTION

Transmissible spongiform encephalopathies or prion diseases are fatal neurodegenerative disorders that include Creutzfeldt–Jakob disease and Gerstmann–Sträussler–Scheinker syndrome in humans, and scrapie, bovine spongiform encephalopathy, and chronic wasting disease in animals. These disorders are characterized by accumulation in the brain of an abnormal isoform of prion protein

[1] Department of Prion Research, Tohoku University Graduate School of Medicine, Sendai, Japan.
[2] Department of Pharmaceutical Care and Health Sciences, Faculty of Pharmaceutical Sciences, Fukuoka University, Fukuoka, Japan.
[3] Department of Drug Design and Drug Delivery, Faculty of Pharmaceutical Sciences, Fukuoka University, Fukuoka, Japan.
[4] Institute of Molecular and Cellular Biosciences, University of Tokyo, Tokyo, Japan.
[5] To whom correspondence should be addressed at Department of Prion Research, Tohoku University Graduate School of Medicine, 2-1 Seiryo-cho, Aoba-ku, Sendai 980-8575, Japan; e-mail: doh-ura@mail.tains.tohoku.ac.jp.

(PrP), which is putatively a main component of pathogens or the pathogen itself, and which is rich in beta-sheet structure and resistant to digestion with proteinase K (Prusiner, 1991). Recent outbreaks of variant Creutzfeldt–Jakob disease and iatrogenic Creutzfeldt–Jakob disease through use of cadaveric growth hormone or dural grafts in younger people have necessitated the development of suitable therapies.

We previously found quinacrine and its derivatives to have potent antiprion activity in prion-infected cells (Doh-Ura *et al.*, 2000; Murakami-Kubo *et al.*, 2004). The common structure of these chemicals, a quinoline ring with a side chain containing a nitrogen atom located at a particular distance from another nitrogen atom in the ring indicates that the chemicals have chelating activity, but the involvement of chelating metals in their antiprion activity has never been confirmed. Quinacrine has been used recently for clinical trials of patients with prion diseases in several countries. Orally administered quinacrine is reportedly effective in transiently improving cognitive functions of patients (Nakajima *et al.*, 2004), but it frequently causes such adverse effects as liver dysfunction. For that reason, either improving its penetration into the brain (the target organ of prion diseases) or reducing its uptake into the liver is suggested for producing more beneficial results (Dohgu *et al.*, 2004).

Here, to obtain more effective antiprion compounds with better brain permeability than quinacrine, we screened chelating chemicals in prion-infected neuroblastoma cells. We investigated the brain permeability of a representative chemical using an *in-vitro* model for the blood–brain barrier.

MATERIALS AND METHODS

Chemicals and Cells

Chemicals used in the study were purchased from Sigma-Aldrich Corp. (St. Louis, MO), Tokyo Kasei Kogyo Co. Ltd. (Tokyo, Japan), and Wako Pure Chemical Industries Ltd. (Osaka, Japan). All chemicals, except for chrysoidine, were dissolved in 100% dimethyl sulfoxide (DMSO), although chrysoidine was dissolved in distilled water.

Acetylated Yellow AB was obtained as follows. Yellow AB was dissolved in dichloromethane and mixed with excess glacial acetic acid. After its complete acetylation was observed by thin layer chromatography, the acetylated product was purified using silica gel column chromatography (dichloromethane/ethyl acetic acid: 9/1 (v/v)). The residual solid was lyophilized and identified as acetylated Yellow AB by both fast atom bombardment mass spectrometry and elemental analysis.

Murine neuroblastoma (NB) cells that had been persistently infected with the scrapie prion strain RML (ScNB cells) (Race *et al.*, 1988) were used for the assay of antiprion activity and grown in Opti-MEM (Invitrogen Corp., CA) containing 10% fetal bovine serum. For the assay of brain endothelial permeability, immortalized endothelial cells from the murine brain capillary (MBEC4 cells) (Tatsuta *et al.*, 1992) were used and grown in DMEM (Invitrogen Corp., CA) containing 10% fetal bovine serum, 100 μg/mL streptomycin, and 100 units/mL penicillin.

Antiprion Activity Assay

Antiprion activity of a chemical was assayed by measuring its 50% inhibition dose (IC_{50}) for abnormal PrP formation in ScNB cells, as described previously (Doh-Ura *et al.*, 2000; Ishikawa *et al.*, 2004). Each chemical was added at designated concentrations when cells were passed at 10% confluency. The final concentration of DMSO in the medium was maintained at less than 0.5%. The cells were allowed to grow to confluence and were lysed with a lysis buffer (0.5% sodium deoxycholate, 0.5% Nonidet P-40, PBS). The lysates were digested with 10 μg/mL proteinase K for 30 min and centrifuged at 100,000 $\times$ *g* for 30 min at 4°C. The pellets were resuspended in the sample loading buffer and boiled. The samples were separated using electrophoresis on a 15% Tris-glycine-SDS-polyacrylamide gel and electroblotted. Detection of PrP was done using an antibody PrP-2B, followed by an alkaline phosphatase-conjugated secondary antibody. Immunoreactive signals were visualized with CDP-Star detection reagent (GE Healthcare Bio-Science, NJ) and were analyzed densitometrically. Three independent assays were performed in each experiment.

Cellular PrP Assay

The total level of normal cellular PrP was assayed similarly in noninfected NB cells treated with a chemical. Briefly, the cells were treated with a chemical as described earlier and lysed with the lysis buffer. Four volumes of the lysate were added to one volume of the five times concentrated sample loading buffer and boiled. Then, the samples were analyzed by immunoblotting as described earlier. The cell surface level of normal cellular PrP was assayed by flow cytometry described previously (Kim *et al.*, 2004). Briefly, NB cells dispersed by the treatment with ice-cold PBS containing 0.1% collagenase (Wako Pure Chemicals, Osaka, Japan) were washed with 0.5% fetal bovine serum in PBS (FBS/PBS) and incubated with an antibody SAF83 (1:500) (SPI-BIO, Massy, France) for 30 min on ice. Cells were washed with FBS/PBS and incubated with goat $F(ab')_2$ fragment antimouse IgG(H + L)-PE (Beckman Coulter, CA) for 30 min. After washing, cells were analyzed using an EPICS XL-ADC flow cytometer (Beckman Coulter, CA).

Surface Plasmon Resonance Assay

Binding assay of a chemical with recombinant PrP was performed using an optical biosensor (Biacore AB, Uppsala, Sweden), as described previously (Kawatake *et al.*, 2006). Briefly, recombinant mouse PrP (amino acids 121–231; PrP121–231) was immobilized on a biosensor chip at a density of *ca.* 3,000 resonance units (RU) using amine coupling. Test chemicals were diluted to 50 μM with the running buffer (3% DMSO in PBS, pH 7.4) and were injected over both the PrP flow cell and the reference at a flow rate of 20 μL/min. The dissociation phase was monitored with injection of the running buffer at a flow rate of 20 μL/min. The flow cell was washed with 10 mM NaOH for 30 s between sample injections. Buffer blanks for double referencing were injected before sample analyses.

Brain Endothelial Permeability Assay

Permeability assay was performed as described previously (Dohgu *et al.*, 2004). Briefly, MBEC4 cells were cultured on the collagen-coated polycarbonate membrane of a Transwell insert (Corning Coster Corp., MA). Before assay, the cells were washed with Krebs–Ringer buffer (118 mM NaCl, 4.7 mM KCl, 1.3 mM $CaCl_2$, 1.2 mM $MgCl_2$, 1.0 mM NaH_2PO_4, 25 mM $NaHCO_3$, 11 mM D-glucose, pH 7.4). Then, the buffer (1.5 mL) was added outside of the insert (abluminal side), and the buffer (0.5 mL) containing 100 μM of a chemical was loaded on the luminal side of the insert. Samples (0.5 mL) were recovered from the abluminal chamber at 10, 20, 30, and 60 min and replaced immediately with fresh Krebs–Ringer buffer. Sodium fluorescein (Na-F, MW 376; Sigma-Aldrich Corp., MO) was used as a paracellular transport marker, and chrysoidine (Tokyo Kasei Kogyo Co. Ltd., Tokyo, Japan) as a test chemical, in addition to quinacrine as a control. The chemical concentration was measured by either determining the fluorescent intensity of Na-F (Ex(λ) 485 nm; Em(λ) 530 nm) and quinacrine (Ex(λ) 450 nm; Em(λ) 530 nm) or determining the absorbance of chrysoidine at 450 nm. The permeability coefficient was calculated using the slope of clearance curve for each chemical obtained during the 60-min period according to the method described by Dehouck *et al.* (Dehouck *et al.*, 1992). Statistical analysis was performed using one-way analysis of variance followed by Tukey–Kramer method for multiple comparisons.

RESULTS

Antiprion Screening *in vitro*

To evaluate functional groups of antiprion chelating chemicals, various chelating chemicals were examined for whether they inhibited abnormal PrP formation in prion-infected ScNB cells. Thirty-five chelating chemicals were analyzed; 11 of them were effective in inhibiting abnormal PrP formation for doses at which cell toxicity was not observed (Tables I and II). Nine of the 11 effective chemicals had a common structure, which consisted of aromatic rings (terminals 1 and 2 in Table II) at both ends of an azo bond. Although both 4-methyl-2-(2-thiazolylazo)phenol and 4-(2-pyridylazo)resorcinol were not effective, they also exhibited this structure, with a thiazole ring and a pyridine ring in the terminal 1 portion, respectively. Their lack of effectiveness might be attributable to cell toxicity, which occurred at lower doses than for chemicals carrying a benzene ring in the terminal 1 portion. On the other hand, all chemicals carrying either a benzene ring or a naphthalene ring in the terminal 2 portion were effective. Therefore, the data suggest that a structure with such an aromatic ring as benzene or naphthalene in either end of an azo bond might be responsible for inhibiting abnormal PrP formation in ScNB cells.

Mechanism of Antiprion Action

We tested whether the effective chemicals cause any alteration of the cellular PrP level in the treated cells because reduction in the cellular PrP level engenders

Table I. Antiprion Activity in ScNB Cells of Chelating Compounds

Compound	IC_{50} (μM)	CM (μM)	Compound	IC_{50} (μM)	CM (μM)
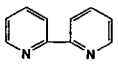	-	75	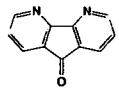	-	>100
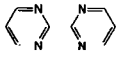	-	>100	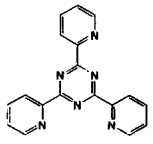	-	25
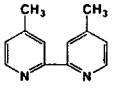	-	10	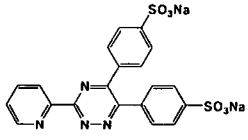	-	>100
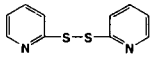	-	10	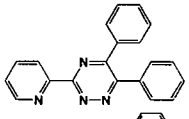	-	10
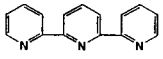	-	0.5	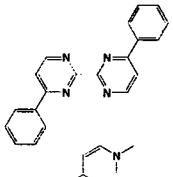	5	25
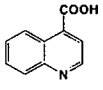	-	>100	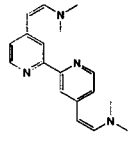	-	5
	-	5	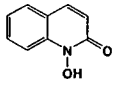	-	25
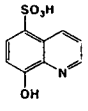	-	>100	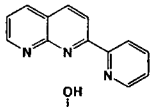	25	>200
	-	5	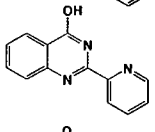	-	10
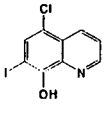	-	10	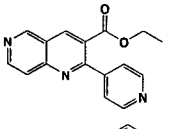	-	>100
			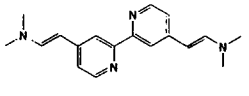	-	5

Note. IC_{50}: approximate dose giving 50% inhibition of abnormal PrP formation relative to the control. CM: approximate maximal dose that does not affect the rate of cell growth to confluence.

Table II. Antiprion Activity in ScNB Cells of Chelating Azo Compounds

Compound	Terminal 1 -N=N-	Terminal 2	IC_{50} (μM)	CM(μM)
Phenylazoresorcinol	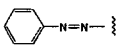		0.3	50
2-Phenylazo-4-methylphenol		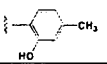	0.3	75
4-Methyl-2-(2-thiazolylazo)phenol	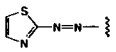		-	0.5
1-(2-Thiazolylazo)-2-naphtol		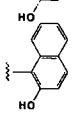	-	0.5
4-(2-Thiazolylazo)resorcinol		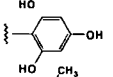	3	5
TAMSMB		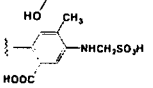	-	>100
4-(2-Pyridylazo)resorcinol	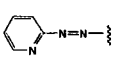		-	0.25
1-(2-Pyridylazo)-2-naphtol		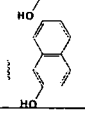	-	1
5-Br-PAPS	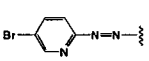	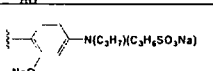	15	20
5-Br-PADAP		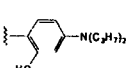	4	10
5-Cl-PADAP	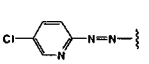	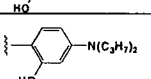	2	5
5-CF_3-PADAP	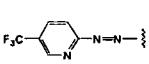	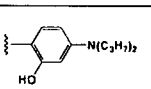	4	10
Yellow AB	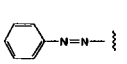	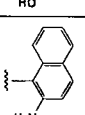	0.5	100
Chrysoidine		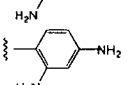	0.015	>100
Congo red	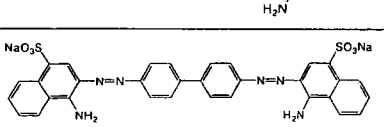		0.014	not tested
Quinacrine	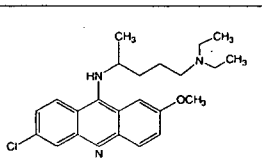		0.4	2

Note. IC_{50}: approximate dose giving 50% inhibition of abnormal PrP formation relative to the control. CM: approximate maximal dose that does not affect the rate of cell growth to confluence. TAMSMB: 4-methyl-5-sulfomethylamino-2-(2-thiazolylazo)benzoic acid. PAPS: 2-(2-pyridylazo)-5-[*N*-*n*-propyl-*N*-(3-sulfopropyl)amino]phenol, disodium salt. PADAP: 2-(2-pyridylazo)-5-diethylaminophenol.

reduction in abnormal PrP formation. The results revealed no reduction in the cellular PrP level of the cells (Fig. 1(A) and (B)). Furthermore, either to examine whether the chemicals directly destabilize or denature the abnormal PrP structure or to exclude the possibility of interference with preparation and immunodetection of the abnormal PrP, the cell lysate either alone or mixed with the chemicals was incubated at 37°C for 1 h prior to proteinase K digestion; it was then processed ordinarily to obtain the abnormal PrP. The results indicated that the chemicals did not affect the abnormal PrP signals (Fig. 1(C)).

Because it was predicted that the chemicals might exert their antiprion action through a certain mechanism involving chelating metals, the most effective chemical found here, chrysoidine, was preincubated before addition to the ScNB culture medium with an equivalent dose or lower doses of various metal ions, including copper, zinc, cobalt, and aluminum ions. The results revealed no change in the inhibition activity of the chemical (Fig. 2). Furthermore, to examine whether chelating activity is necessary for antiprion action, we modified Yellow AB in such a manner that its amino base was acetylated to remove its chelating activity. The acetylated Yellow AB was tested in ScNB cells, and it was one-eighth as effective in inhibiting abnormal PrP formation as Yellow AB (Fig. 3(A)). Finally, as a chemical bearing the effective structure but lacking chelating activity, the chemical azobenzene, which is most similar in the structure to the chemical chrysoidine, was tested. It was about 30 times less effective than chrysoidine (Fig. 3(B)). These findings suggest that chelating activity is not essential for the antiprion action but might influence it.

Interaction with Recombinant PrP

We previously reported that more potent antiprion agents have higher affinity to recombinant PrP121–231 in surface plasmon resonance (SPR) analysis (Kawatake *et al.*, 2006). Therefore, we examined whether this is also demonstrated in the effective chelating chemicals found here. Six of the chemicals (each at 50 μM) were tested. The SPR sensorgrams of the chemicals except 4-(2-pyridylazo)resorcinol showed similarly weak signal responses of less than 100 RU as quinacrine did (Fig. 4). However, neither 4-(2-thiazolylazo)resorcinol nor Yellow AB reached the equilibrium state at the association phase; neither 4-(2-thiazolylazo)resorcinol nor 2-phenylazo-4-methylphenol returned to the baseline at the dissociation phase. In contrast, 4-(2-pyridylazo)resorcinol showed the strongest response of more than 200 RU and neither reached the equilibrium state at the association phase nor returned to the baseline at the dissociation phase. The binding response value from the sensorgram (equilibrium or maximum response value divided by molecular weight), which is an index for estimating the interaction of a chemical with the molecules sited on a biosensor chip (Frostell-Karlsson *et al.*, 2000), showed no apparent relationship with the IC_{50} value of antiprion activity (data not shown), suggesting that the chemicals found here might exert their antiprion action in a manner that differs from those of previously reported antiprion chemicals such as antimalarias and amyloid binding dyes.

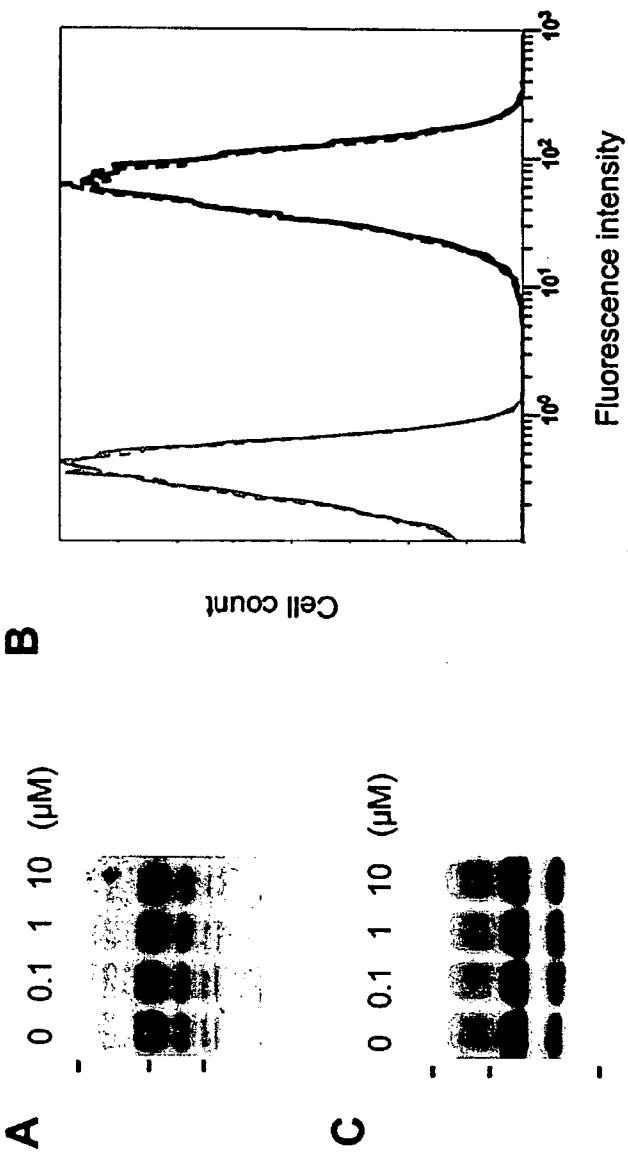

Fig. 1. Effects of a representative chemical, chrysoidine, on the cellular PrP (A, B) and the cell lysate abnormal PrP (C). (A) Immunoblot data of the total cellular PrP in noninfected NB cells treated with a designated dose of chrysoidine. *Bars* on the *left* indicate molecular size markers at 81, 42, and 32 kDa. (B) Flow cytometry data of the cell surface PrP in noninfected NB cells treated with 1 μM chrysoidine. *Solid line* and *broken line* indicate chrysoidine-treated cells and nontreated cells, respectively. *Grey line* peaks on the *left* show their respective isotype controls. (C) Immunoblot data of the abnormal PrP from ScNB cell lysate preincubated with a designated dose of chrysoidine prior to protease digestion. Molecular size markers on the left are 42, 32, and 18 kDa.

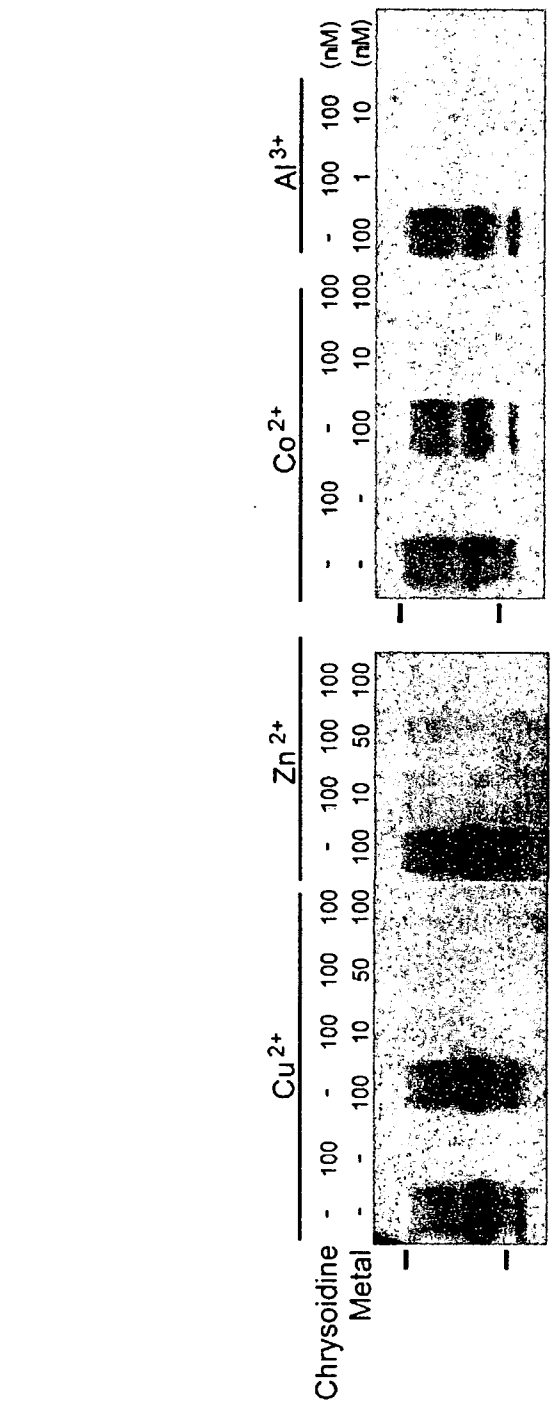

Fig. 2. Antiprion activity in ScNB cells of chrysoidine preincubated with metal ions. Immunoblot data of the abnormal PrP are shown. *Bars* on the *left* indicate molecular size markers at 37 and 25 kDa.

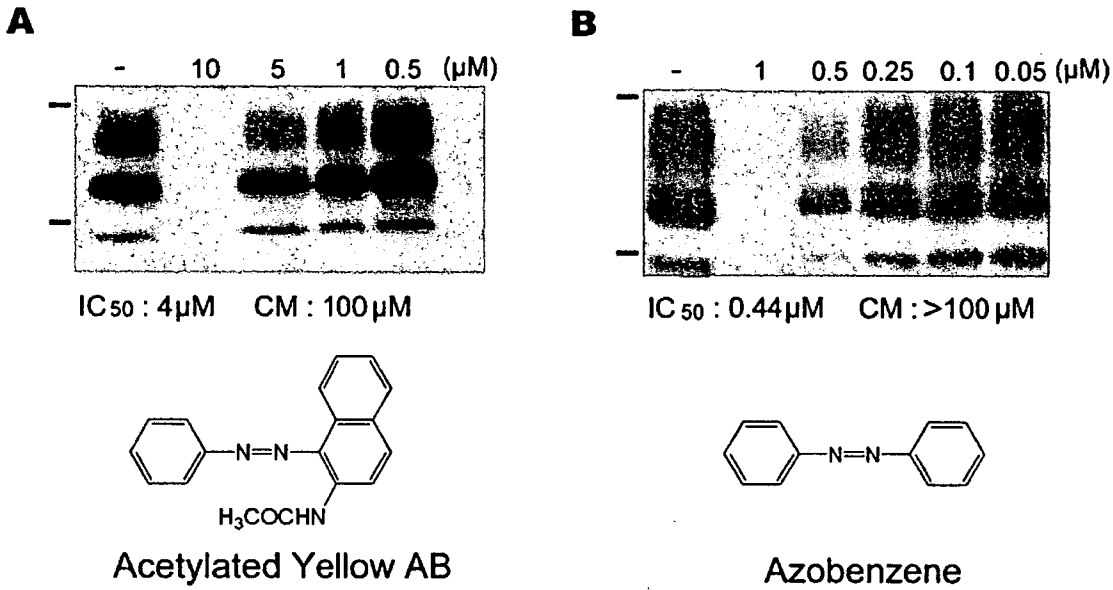

Fig. 3. Antiprion activity in ScNB cells of acetylated Yellow AB (A) and azobenzene (B) Immunoblot data of the abnormal PrP are shown. *Bars* on the *left* indicate molecular size markers at 37 and 25 kDa. IC_{50} is approximate dose giving 50% inhibition of abnormal PrP formation. CM is approximate maximal dose that does not affect the rate of cell growth.

Brain Endothelial Permeability

The brain is the main organ that is affected in prion diseases. Therefore, therapeutic compounds must penetrate into the brain. To examine the permeability of a chemical through the blood–brain barrier, we used a simple analytical model consisting of brain capillary endothelial MBEC4 cells. As a representative of the effective chemicals found in the study, chrysoidine was examined in this model and compared with a paracellular marker, Na-F, as well as a control, quinacrine, which has been used for clinical trials of patients with prion diseases. The results showed that the respective permeability coefficients of Na-F, quinacrine, and chrysoidine were 2.17×10^{-3}, 0.96×10^{-3}, and 4.63×10^{-3} cm/min (Fig. 5). Therefore, chrysoidine penetrated the brain capillary endothelial cells about five times more efficiently than quinacrine.

DISCUSSION

Here, we revealed that chelating chemicals, especially aromatic azo compounds, have antiprion activity. Mechanisms of their antiprion action apparently include neither alteration of cellular PrP level nor direct modification of abnormal PrP. Taken together with previous findings related to the interaction of PrP with metals (review in Brown, 2004), the data obtained through the present study suggest that the chelating activity might influence the antiprion action but is not essential for

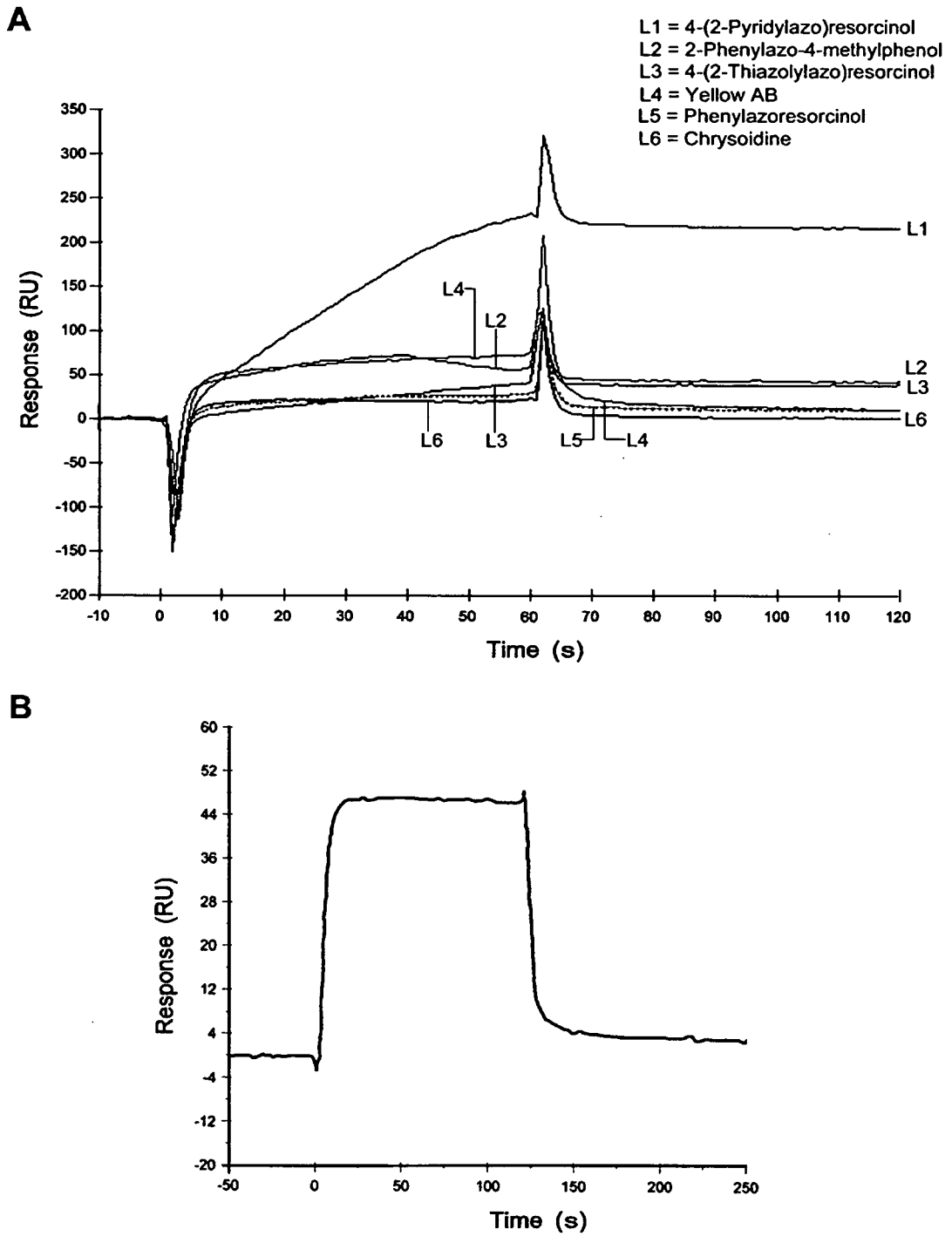

Fig. 4. SPR sensorgrams of chelating compounds (A) and quinacrine (B) interacting with PrP121–231.Each chemical at 50 μM was analyzed using a *ca.* 3,000 RU PrP-bound biosensor chip. Each phase of association and dissociation was monitored for 60 s in (A) or 125 s in (B).

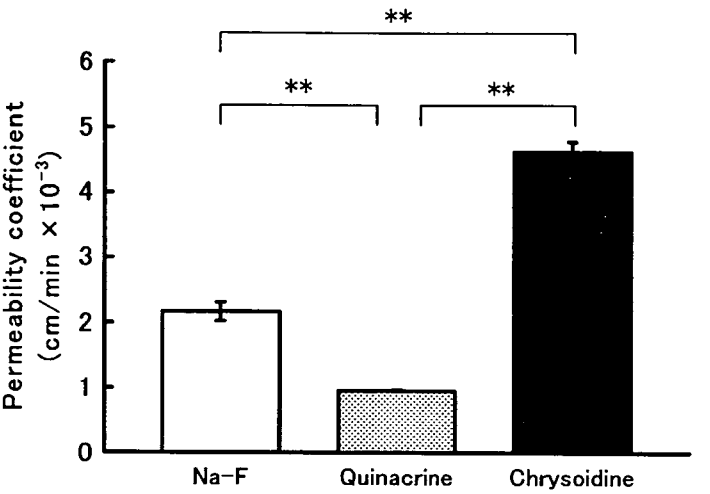

Fig. 5. Permeability coefficients of Na-F, quinacrine, and chrysoidine through MBEC4 monolayer. Each chemical at 100 μM was analyzed. The values are mean ± SEM (n = 3–4 inserts). $^{**}p < 0.01$; significant difference between each group.

it. This inference is consistent with our previous results from quinacrine derivatives carrying chelating activities (Murakami-Kubo *et al.*, 2004).

Chrysoidine, a representative chemical found in this study, is far superior to quinacrine in both the antiprion activity and the brain endothelial permeability. The respective antiprion activities of chrysoidine and quinacrine in ScNB cells were 15 nM and 400 nM in IC_{50}, indicating that chrysoidine is about 27 times more effective than quinacrine. Furthermore, chrysoidine penetrated brain capillary endothelial cells about five times more efficiently than quinacrine. In addition, chrysoidine is much less toxic than quinacrine because a maximal dose at which the ScNB cell growth to confluence is still tolerant was more than 100 μM in chrysoidine or 2 μM in quinacrine (Table II). These findings suggest that chrysoidine might be more beneficial *in vivo* than quinacrine, but the *in vivo* efficacy of chrysoidine remains to be evaluated.

Results from the SPR analysis obtained here were not consistent with those of our previous study (Kawatake *et al.*, 2006), where the SPR binding response correlates with the inhibition activity of abnormal PrP formation in ScNB cells. Chrysoidine, the most effective chemical in the study, has a similar structure to either half of a symmetrical compound, Congo red, whose antiprion activity (IC_{50} = 14 nM) is as prominent as that of chrysoidine (IC_{50} = 15 nM) (Table II) but whose permeability into the brain is reportedly very poor because of low lipophilicity and high charge in its acidic groups (Klunk *et al.*, 2002). Interaction with recombinant PrP121–231 differs greatly between chrysoidine and Congo red. Congo red has very high affinity (K_D = 1.6 μM) and strong binding response (1.7 RU/Da at 10 μM using a *ca.* 3,000 RU PrP-bound biosensor chip) to the PrP121–231 (Kawatake *et al.*, 2006), whereas chrysoidine shows a sensorgram pattern of low affinity compounds and has very low binding response (0.1 RU/Da at 50 μM using a similar

biosensor chip). These facts suggest that chrysoidine exerts its antiprion action in a manner that differs from that of Congo red, but this inference demands further evaluation.

The brain endothelial permeability assay using MBEC4 cells revealed that the permeability coefficient of quinacrine was much lower than that of Na-F. The results are consistent with those of our previous experiments (Dohgu *et al.*, 2004). Quinacrine transport through the blood–brain barrier is mediated by both the efflux system (P-glycoproteins) and the influx system (organic cation transporter-like machinery). Therefore, quinacrine entry into the brain is controlled by three factors: P-glycoprotein-mediated active efflux at the apical side of the plasma membrane; highly concentrative uptake system; large storage capacity in the cytoplasm of the brain endothelial cells. On the contrary, Na-F is transported through paracellular routes (tight junctions) at the blood–brain barrier, and neither active efflux nor concentrative uptake system is involved in the Na-F permeability. These differences might explain the reason why quinacrine is less efficiently permeabilized than Na-F.

Chrysoidine is used in various fields as a yellowish fluorescent dye. This chemical was suggested to relate with bladder cancer in humans (Cartwright *et al.*, 1983; Sole and Sorahan, 1985), but it is still controversial because the data of a later conducted case-control study denied its relation to the cancer (Sorahan and Sole, 1990). There are no data on the genetic and related effects of the chemical in humans, but it is mutagenic to bacteria and toxic to rat hepatocytes *in vitro* (Sandhu and Chipman, 1990). In the mice orally administered, it produced liver carcinoma, leukemia, and reticulum cell sarcomas (Anonymous, 1975). These findings suggest that clinical use of chrysoidine or related chemicals might be inadequate.

In conclusion, we screened chelating chemicals and found that chrysoidine was much more effective in both antiprion activity and brain endothelial permeability than quinacrine, and it was much less toxic in NB cells. The mechanism of antiprion action of this compound did not apparently include alteration of cellular PrP level, direct modification of abnormal PrP, or chelation of metals. Its interaction with PrP121–231 differed greatly from that of Congo red, despite their structural similarity. These findings will contribute to the development of therapeutic compounds for prion diseases.

ACKNOWLEDGMENTS

This study was supported by a Grant (H16-kokoro-024) to K.D. from the Ministry of Health, Labor, and Welfare, Japan. The authors thank Drs. Jiro Takata, Atsushi Yamauchi, Shinya Dohgu, Satoshi Kawatake, Toru Iwaki, and Kenta Teruya for their suggestions, and Ms. Kyomi Sasaki for manuscript preparation.

REFERENCES

Anomymous. (1975). Chrysoidine. *Int. Agency Res. Cancer Monogr.* **8**:91–96.
Brown, D. R. (2004). Metallic prions. *Biochem. Soc. Symp.* **71**:193–202.